Type of article: Original Article

Evaluate the efficiency of Mr BMT in macrophage replacement of peripheral organs

Jinjin Du [1,3,#], Baozhi Yang [1,2,#], Yang He [3*], Yanxia Rao [2*]

Author affiliations:

[1] School of Basic Medical Sciences, Jinzhou Medical University, Jinzhou, Liaoning 121001, China

[2] Department of Neurology, Zhongshan Hospital, Department of Laboratory Animal Science, MOE Frontiers Center for Brain Science, Fudan University, Shanghai 200032, China

[3] Institute for Translational Brain Research, State Key Laboratory of Medical Neurobiology, MOE Frontier Center for Brain Science, Fudan University, Shanghai

[#] These authors contribute equally.

* Correspondence: 21111520009@m.fudan.edu.cn (Y.H.), yanxiarao@connect.hku.hk (Y.R.)

Total number of pages: 32

Total number of photographs: 8

Word counts: for abstract: 181, for the text: 4059

Competing Interests

The authors declare no competing financial interests.

Evaluate the efficiency of Mr BMT in macrophage replacement of peripheral organs

Abstract

The successful replacement of endogenous tissue-resident macrophages with healthy bone marrow-derived cells through transplantation presents a promising therapeutic approach for treating disease associated with macrophage dysfunction. Our previous development of the novel microglia replacement by bone marrow transplantation (Mr BMT) method achieved high engraftment efficiency in the central nervous system (CNS), overcoming the limitation of traditional bone marrow transplantation (tBMT). In this study, we aimed to investigate the potential impacts of Mr BMT approach on peripheral organs. The Mr BMT approach involves depleting resident microglia through colony stimulating factor-1 receptor (CSF-1R) inhibition, so we first evaluated the survival of peripheral macrophages after CSF-1R inhibition. We observed that the CSF-1R antagonist, PLX5622, exerted significant elimination of peripheral tissue macrophages, albeit with lower efficiency than in the CNS. Furthermore, we discovered that Mr BMT achieved replacement efficiencies comparable to tBMT in peripheral tissues such as the liver, kidney, lung, and spleen. Our findings suggested Mr BMT is a highly efficient strategy for allogeneic macrophage replacement in both the CNS and peripheral organs, and it could have potential clinical applications.

Key-words: microglia, macrophage, microglia replacement, Mr BMT, tBMT, CSF-1R

45 ***Introduction***

46 Tissue-resident macrophages, including microglia which are brain parenchyma resident macrophages,
47 continuously monitor and clear pathogens throughout the lifespan. The new paradigm suggests that
48 several tissue-resident macrophage populations are seeded during waves of embryonic haematopoiesis
49 and self-maintain independently of BM contribution during adulthood[1-3]. Microglia and other
50 tissue-resident macrophages play essential roles in the development, homeostasis, tissue repair, and
51 disease defence both in the CNS and peripheral organs. Dysfunction or genetic mutations have been
52 linked to a wide range of diseases, including neurodegeneration, autoimmune disorders, inflammation,
53 and bone disease[4]. Allogeneic bone marrow and stem cell transplantation are effective options for
54 the treatment of inherited diseases of the immune system, such as severe combined immunodeficiency
55 (SCID)[5] and some autoimmune diseases, including systemic lupus erythematosus (SLE)[6] ,
56 rheumatoid arthritis (RA)[7] , type 1 diabetes (T1D)[8] and multiple sclerosis (MS)[9] . This approach
57 involves replacing the recipient's bone marrow and immune cells with healthy donor cells that can
58 repopulate the immune system, leading to improved disease outcomes.

59

60 We previously developed a novel strategy for nonself microglia replacement by bone marrow
61 transplantation at CNS-wide scale and named this procedure Mr BMT[10] . This involves first
62 depleting the resident microglia through either genetic or pharmacological means, followed by
63 transplantation of bone marrow cells that giving rise to new microglia. The existing microglia of
64 recipient mice will be replaced by microglia-like cell derived from bone marrow cells[11, 12] . This
65 strategy can be useful in cases where the resident microglia are dysfunctional and contribute to the
66 development of neurodegenerative, such as Alzheimer’s disease (AD)[13] , Parkinson disease (PD)[14]
67 and Frontotemporal dementia (FTD)[15] . However, it is important to evaluate the potential effects of
68 Mr BMT on peripheral tissue macrophages when considering this therapy for clinical translation, since

69 the approach used for microglia ablation also have significant effects on the tissue macrophages and
70 monocyte populations[16-18].
71
72 The current study observed highly effective tissue macrophage replacement in the liver, kidney, lung,
73 and spleen after Mr BMT, indicating the potential of this therapy to have broad impacts on tissue
74 macrophage populations throughout the peripheral organs. These encouraging results suggested that
75 Mr BMT may be a promising cell therapy strategy for a wide range of diseases that affect both the
76 central and peripheral immune systems, such as amyotrophic lateral sclerosis (ALS) and
77 adrenoleukodystrophy (ALD).
78
79 ***Materials and Methods***
80 **Animals and PLX5622 administration**
81 *Cx3cr1*-GFP (B6.129P2(Cg)-*Cx3cr1*^{tm1Litt}/J, Strain #: 005582) mice were purchased from the Jackson
82 Laboratory (Shanghai, China)[19]. C57BL/6J mice were purchased from Charles River (Shanghai,
83 China). All mice were housed in the Animal Facility at the Department of Laboratory Animal Science
84 at Fudan University under a 12 hours light/dark cycle with food and water given ad libitum. All animal
85 experiments were conducted in accordance with the guidelines of the Institutional Animal Care and
86 Use Committee of the Department of Laboratory Animal Science at Fudan University (202009001S
87 and 2021JS-NZHY-002). All PLX5622 were formulated in AIN-76A chow at a concentration of 1200
88 mg/kg (Cat# D20010801, SYSE Bio, Changzhou, China). PLX5622 group mice were fed with
89 PLX5622 chow for 14 days ad libitum. Control diet group mice were fed with AIN-76A chow ad
90 libitum.
91
92 **Tissue preparation for the cryosection and immunohistochemistry**

93 Mice were deeply anesthetized with isoflurane and were then subjected to transcranial perfusion with
94 50 ml of 0.01 M cold PBS or 0.9% NaCl. Next, all mice were perfused with 4% cold paraformaldehyde
95 (PFA) for fixation. The brains and peripheral organs, including liver, lung, kidney and spleen were
96 collected and postfixed in 4% PFA overnight (ON) at 4 °C or 6 hours in room temperature (RT). All
97 tissues were dehydrated by 30% sucrose in 0.01 M PBS in 4 °C for 2-3 days and then embedded in
98 optimal cutting temperature compound (OCT). All samples were stored at -80 °C before cryosection.
99 All tissues were frozen in the freezing microtome for 15 minutes before cryosection. Tissues with
100 regions of interest were sectioned by Leica CM1950 cryostat at 35 μm thickness.
101

102 **Immunohistochemistry and image acquisition**

103 The sections of brain and peripheral organs were rinsed by 0.01 M PBS for 3 times. Next, brain and
104 peripheral organ sections were blocked and permeabilized with 0.01 M PBS containing 0.03% Triton
105 X-100 and 4% normal donkey serum (NDS) for 2 hours at RT. Next, the samples were incubated in
106 primary antibody in 1% NDS in PBST at 4 °C ON. After rinsed by 0.03% PBST for 3 times, the
107 samples were incubated fluorescent dyes conjugated secondary antibody in 1% NDS in PBST for 2
108 hours at RT, together with 1:500 4', 6-diamidino-2-phenylindole (DAPI). Next, samples were rinsed
109 by 0.03% PBST for 3 times and then mounted anti-fade mounting medium. The edge of the cover glass
110 was sealed with nail enamel.
111 Primary antibody information and concentration: rabbit anti-IBA1 (1:500, Cat# 019-19741, Wako,
112 Japan); goat anti-IBA1 (1:500, Cat# ab5076, Abcam, Cambridge, UK); goat anti-GFP (1:1000, Cat#
113 ab6673, Abcam, Cambridge, UK); rabbit anti-GFP (1:1000, Cat# A11122, Thermo Fisher,
114 Massachusetts, USA); rat anti-F4/80 (1:500, Biolegend, Cat# 123101, California, USA); mouse anti-
115 CD11c (1:500, Cat# 117314, Biolegend, California, USA). Secondary antibody information: Donkey
116 anti-rat 647 (1:1000, Cat# A48272, Invitrogen, California, USA); Donkey anti-rat 568 (1:1000, Cat#
117 ab175475, Abcam, Cambridge, UK); Donkey anti-rabbit 488 (1:1000, Cat# A11008, Thermo Fisher,

118 Massachusetts, USA); Donkey anti-goat 488 (1:1000, Cat# A11055, Thermo Fisher, Massachusetts,
119 USA); Donkey anti-rabbit 568 (1:1000, Cat# A10042, Thermo Fisher, Massachusetts, USA); Donkey
120 anti-rabbit 647 (1:1000, Cat# 711-605-152, Jackson, Pennsylvania, USA).
121 Confocal images were acquired by using an Olympus FV3000 confocal microscope with a solid- state
122 laser. Lasers with wavelengths of 405 nm, 488 nm, 561 nm, and 640 nm were used to excite the
123 fluorophores. Then, ×60 (oil), ×40 (oil), and ×20 objectives were utilized. Some whole-brain
124 fluorescence images were acquired by an Olympus VS120 microscope equipped with a motorized
125 stage. Then, ×10 objective was used. Z-stacked focal planes were acquired and maximally projected
126 with Fiji. The brightness and contrast of the image were adjusted with Fiji if necessary.
127
128 **Bone marrow cells preparation**
129 Bone marrow cells were collected from adult *Cx3cr1*$^{+/GFP}$ mice. In brief, femora and tibia were
130 collected and the muscles were removed. Next, the bones were placed in cold 0.01 M PBS and washed
131 twice. After that, bone marrow cells were collected using 10 mL syringe with a 26-gague needle. Next,
132 cells were washed by L15 medium containing 10% FBS and centrifuged at 300 g for 10 minutes. Cell
133 pellets were then resuspended with L15 medium containing 10% FBS and passed through 40 μm cell
134 strainers. After that, cell number was counted, and bone marrow cells were diluted in appropriate
135 amount medium for downstream applications.
136
137 **Traditional bone marrow transplantation (tBMT)**
138 The tBMT was carried out according to our previous description with some modifications[10]. Briefly,
139 adult recipient C57BL/6J mice were fed with acid water (PH=2~3) and neomycin (1.1 g/L) for 14 days
140 till receiving 9 Gy X ray treatment. After irradiation, the recipient mice were administrated with GFP-
141 labelled 1×10^7 bone marrow cells from the donor through tail vein injection.
142

143 **Microglia replacement by bone marrow transplantation (Mr BMT)**

144 The Mr BMT was carried out according to our previous description with some modifications[20]. In
145 brief, adult recipient C57BL/6J mice were administrated PLX5622 together with acid water (PH=2~3)
146 and neomycin (1.1 g/L) for 2 weeks till receiving 9 Gy X ray treatment. At the same day, the recipient
147 mice were intravenous administrated with GFP-labelled 1×10^7 bone marrow cells from the donor
148 through tail vein injection.

149

150 **Statistical analysis**

151 Statistical analyses were conducted using Prism 9 (GraphPad). Each data point represented the average
152 statistical result of three sections in different regions of brain, liver, kidney, lung and spleen. Results
153 were determined independently in double-blind manner. Data were presented as mean ± standard
154 deviation (SD). One-way analysis of variance (ANOVA) with Holm-Sidak's multiple comparisons
155 test (post hoc) was performed for multiple comparisons, while unpaired t test was performed to
156 compare the differences between two groups, unless otherwise stated. Statistical significance was set
157 as $p < 0.05$.

158

159 ***Results***

160 **CSF-1R inhibitor-induced elimination of tissue macrophages**

161 The colony stimulating factor-1 (CSF-1) signalling pathway is known to regulate the development,
162 proliferation, migration, function and survival of myeloid cells, including microglia and peripheral
163 tissue macrophages[21]. The PI3K/Akt pathway has a central role in CSF-1R mediated macrophage
164 survival. In macrophages, Akt can be activated directly through the CSF-1R pTyr721/PI3K
165 pathway and indirectly by ceramide-1-phosphate (C1P) or the Gab2/PI3K pathway, which is
166 counterbalanced by a CSF-1R pTyr559/LynSHIP-1 pathway[22]. Previous study showed that the
167 inhibition of CSF-1R would result in the elimination of microglia in the adult brain and the

168 establishment of a microglia-free niche[23]. Meanwhile, the survival of peripheral tissue-resident
169 macrophages and monocyte are also threatened[18]. Additionally, interference with CSF-1R signalling
170 through depleting *Csf1r* enhancer can lead to the lack of myeloid cells, including the microglia in brain
171 and macrophages in skin, kidney, heart, and peritoneum. However, the other periphery tissue
172 macrophages are unaffected[24].
173
174 The small molecule PLX5622 is a CSF-1R antagonist that has been tested in a range of animal
175 models[23, 25, 26]. Here, adult mice were administered control and PLX5622 chow for 14 days to
176 examine whether CSF-1R inhibition could generate a macrophage-free niche in peripheral tissues
177 within this time window (Fig. 1A). IBA1 was used as a marker to determine the number of microglia
178 in brain and macrophages in peripheral organs, as IBA1 is specifically expressed in most
179 subpopulations of monocyte and macrophage lineage cells[27]. Consistent with previous studies, we
180 observed that PLX5622 treatment resulted in the elimination of ~99% of microglia and the creation of
181 a microglia-free environment in the brain[23]. However, unlike with the observation in brain, 44.08%
182 IBA1-positive macrophages were depleted in the liver, 50.58% in the lung, 87.123% in the kidney,
183 31.41% in the spleen after 14 days PLX5622 treatment (Fig. 1B and Fig. S1). These observations
184 demonstrated that PLX5622 exerted a significant elimination of peripheral tissue macrophages,
185 although its efficiency was lower than in the CNS.
186
187 Although F4/80 is widely used in the analysis of macrophages, it is also expressed in other immune
188 cells, such as dendritic cells (DCs) in the spleen[28]. We evaluated the co-expression rate of F4/80 and
189 IBA1 in various tissues. Our results showed that all F4/80^{+} cells expressed IBA1 in the liver, but 85.67%
190 F4/80^{+} cells expressed IBA1 in the lung, and 50.17% in the kidney, 92.96% in the spleen (Fig. S2).
191 Additionally, the elimination rate of F4/80-positive cells after PLX5622 treatment varied among
192 tissues, with 44.08% in the liver, 51.62 % in the lung, 97.46% in the kidney, and 36% in the spleen

193 (Fig. 1C and 1D). Interestingly, the absent of F4/80^{+} macrophages in kidney after CSF-1R antagonist
194 treatment was consistent with the findings in *Csf1* enhancer deletion mice[29]. Noticeably,
195 granulocyte-macrophage colony stimulating factor 2 (GM-CSF) , also known as colony stimulating
196 factor-2 (CSF-2) regulates lung macrophage survival together with CSF-1[30]. CSF-2/CSF2RB
197 signalling pathway is also important for alveolar macrophage survival, so inhibiting CSF-1R alone
198 will not kill all alveolar macrophages. As CSF-1/CSF-1R signal pathway is crucial for the proliferation
199 and survival of patrolling monocytes[31, 32], the declined number of IBA1 and F4/80 cells in the lung
200 after PLX5622 administration was also likely attributed to the elimination of monocytes.
201
202 **Mr BMT successfully replaced Kupffer cells with BM-derived macrophages in the liver**
203 We previously discovered that microglia-free niche is a prerequisite condition for the successful
204 engraftment of BM-derived cells[10]. We thus hypothesized that the elimination of tissue macrophages
205 by utilization of CSF-1R inhibitor would improve the BM engraftment efficiency. To evaluate the
206 replacement efficiency of macrophages in the liver, we used *Cx3cr1*$^{+/GFP}$ mice as donor, as CX3CR1
207 is expressed in monocyte/macrophage lineage cells[19]. The recipient mice were fed with PLX5622-
208 formulated chow for 14 days and then subjected to X-ray irradiation, followed by an intravenous
209 injection of 1×10^{7} BMCs from *Cx3cr1*$^{+/GFP}$ as we previously described[11]. After that, the recipient
210 mice were fed with control diet for thirty days to remove the CSF-1R inhibition (Fig. 2A). We replaced
211 98.62% of brain resident microglia with BM-derived microglia-like cells (Fig. S3), indicating that Mr
212 BMT exhibits an exceptionally high level of transplantation effectiveness within the brain. We firstly
213 examined BM-derived macrophages ratio in the peripheral organs of the chimeric mouse, then the
214 morphological changes were also included in the analysis.
215
216 In the adult mouse liver, Kupffer cells (KCs) are originated from yolk sac (YS) and fetal liver
217 monocyte-derived macrophages and replenished independently by monocyte-derived precursors in the

218 steady state[1]. Both cell populations share common macrophage functions, including phagocytosis,
219 pathogen defence, native and adaptive immune regulation. Here, we observed that more than 98.22%
220 of primary KCs were replaced by BM-derived $GFP^{+}IBA1^{+}$ macrophages at thirty days post Mr BMT.
221 There was no significant difference in transplantation efficiency between tBMT and Mr BMT (Fig.
222 2B-2D). Compared with primary KCs, the body size of the BM-derived KCs was smaller, implying
223 different cell originations of KCs are linked to the discrepancies in cell morphology and function like
224 immune response and tissue repairment ability (Fig. 2E and 2F).
225
226 **Mr BMT strategy showed high replacement efficiency of kidney tissue macrophages**
227 We further tested the macrophage replacement efficiency in the kidney after tBMT and Mr BMT. In
228 the renal, the majority tissue macrophages are derived from YS and fetal liver macrophages, and the
229 YS derived macrophages progressively expand in the mouse kidney with age[33]. These populations
230 are maintained in situ by self-renewal, largely independent of adult haematopoiesis across lifespan[34,
231 35]. Immunofluorescent (IF) staining of GFP in kidney sections from recipient C57BL/6J mice
232 revealed GFP^{+} BM-derived macrophages spread out the cortex and medulla after tBMT and Mr BMT
233 (Fig. 3A). About 87.22% of tissue macrophages were reconstituted by $GFP^{+}IBA1^{+}$ BM-derived
234 macrophages thirty days after tBMT (Fig. 3B and 3C). After recovery from Mr BMT, more than 87.50%
235 of primary kidney macrophages were successfully colonized by $GFP^{+}IBA1^{+}$ BM-derived macrophages
236 (Fig. 3B-3C), suggesting Mr BMT achieved a similar replacement efficiency to tBMT. Both in tBMT
237 and Mr BMT group, the replacement rate of $GFP^{+}F4/80^{+}$ / $F4/80^{+}$ was similar to $GFP^{+}IBA1^{+}$ / $IBA1^{+}$
238 (Fig. 3B-3D). Previous study demonstrated the endogenic macrophages presented a distinct
239 morphology and function compared to BM-derived macrophages[20, 36, 37]. Therefore, we examined
240 the morphology of the newly formed macrophages in the kidney after tBMT and Mr BMT. We
241 observed that the surface area was reduced significantly in BM-derived macrophages, implying BM-
242 macrophages did not fully acquire a resident macrophage phenotype (Fig. 3E and 3F).

243

244 **Mr BMT achieved high engraftment efficiency of macrophages in the lung and spleen**

245 Next, we examined the profile of BM-originated macrophages in the lung either after tBMT or Mr
246 BMT (Fig. 4A). After transplantation, a great number of GFP^+ BM-derived cells proliferated in the
247 recipient mouse lung, and subpopulations of them were labelled by macrophage/monocyte lineage
248 marker IBA1 and F4/80. After recovery from tBMT, about 80.70% endogenous
249 macrophages/monocytes cells were replaced by GFP^+ $F4/80^+$ BM cells. In Mr BMT group, there were
250 85.17% $IBA1^+$ and 76.53% $F4/80^+$ cells in the recipient mouse lung were detected as BM-derived
251 GFP^+ cells after Mr BMT (Fig. 4B-4D), suggesting comparable replacement efficiency to tBMT.
252 Previous study has demonstrated that $CX3CR1^+$ BMCs could give rise to DCs and supply tissue DCs
253 in lung[38, 39]. We found 2.81% of GFP^+ cells that were $IBA1^-$ and $F4/80^-$, which were likely to
254 differentiate into pulmonary DCs (Fig. 4E and 4F). Lung resident macrophage contained alveolar
255 macrophages (AMs) and interstitial macrophages (IMs)[40]. AMs have high expression of CD11c and
256 low expression of CX3CR1[41, 42], which is totally different from the GFP^+ cells after tBMT or Mr
257 BMT. Thus, we hypothesized that the replacement cells more likely to convert to IMs after thirty days
258 recovery.

259

260 Lastly, we investigated the replacement efficiency of macrophages/monocytes in the spleen after
261 received *Cx3cr1*$^{+/GFP}$ transplantation (Fig. 5A). Regardless of the approaches used for BMT, the
262 staining results revealed that more than 50% of tissue-resident macrophages were replaced by GFP^+
263 BM-derived cells (Fig. 5B-5D). Compared with other peripheral organs, the replacement rate in the
264 spleen was lower, which may be attributed to the different macrophage turnover rate in different organs.
265 However, similar with the observations in other peripheral organs, BM-derived macrophages in the
266 spleen possessed a smaller cell body and less branches, differing from the endogenous embryonic

267 originated macrophages. Additionally, there are 6.96 % GFP^+ cells that were $IBA1^-$ and $F4/80^-$, which
268 were likely to contribute to DCs in the spleen (Fig. 5E and 5F).
269
270 ***Discussion***
271 The Mr BMT approaches a highly efficient strategy for the replenishment of endogenous microglia
272 with BM-derived microglia-like cells at the CNS-wide scale (over 92%) in adult mouse. In contrast,
273 BMCs do not extensively proliferate and engraft the recipient brain (less than 5~20%) by using tBMT
274 method. In current study, we further investigated tissue-resident macrophages replacement efficiency
275 in the peripheral organs by using the Mr BMT approach. Our results demonstrated that BM-derived
276 macrophages efficiently reconstituted tissue macrophages in the liver, kidney, lung and spleen.
277 Although the replacement efficiency had a subtle difference in different organs, which may be
278 attributed to the different turnover rate of tissue-resident macrophages. Thus, Mr BMT achieved a
279 similarly high replacement efficiency comparable to tBMT, but owned higher efficiently in the CNS.
280 These findings suggested that the Mr BMT approach could be a powerful tool for allogenic
281 macrophages replacement in both CNS and peripheral organs. It means that Mr BMT may be a
282 promising cell therapy strategy for a wide range of diseases that affect both central and peripheral
283 myeloid cells, such as ALS and ALD. Despite these encouraging findings, it is important to fully
284 understand the safety of Mr BMT, including its potential long-term effects on tissue macrophage
285 populations and any risks associated with the irradiation used for myelosuppression. Nonetheless, with
286 continued research and development, the Mr BMT strategy may ultimately offer a powerful tool for
287 the treatment of a range of diseases that affect the immune system.
288
289 **Ethics approval and consent to participate**
290 All animal experiments were conducted in accordance with the guidelines of the Institutional Animal
291 Care and Use Committee of the Department of Laboratory Animal Science at Fudan University (permit

number: 202110005S).

Declaration of Competing Interest

The authors have no commercial, proprietary or financial interest in the products or companies described in this article.

Author contributions

Y.R. supervised and conceptualized this study. Y.R., and B.Y. wrote the manuscript. B.Y. and Y.H. performed most experiments. B.Y. analysed the staining results, J.D. and Y.H. provided necessary study support. All authors discussed the results and commented on this manuscript. And at last, we appreciate Open AI's assistance in language.

Acknowledgements

The authors thank Yanxia Rao and Bo Peng (Fudan University) for their sponsorship and support of this experiment. Fang Lei and Jiachen Zhu (Fudan University) for the excellent laboratory management. In addition, the authors express their gratitude and respect to all animals sacrificed in this study.

Data Availability Statement:

The raw data supporting the conclusion of this article will be made available by the authors, without undue reservation.

Figures and Tables:

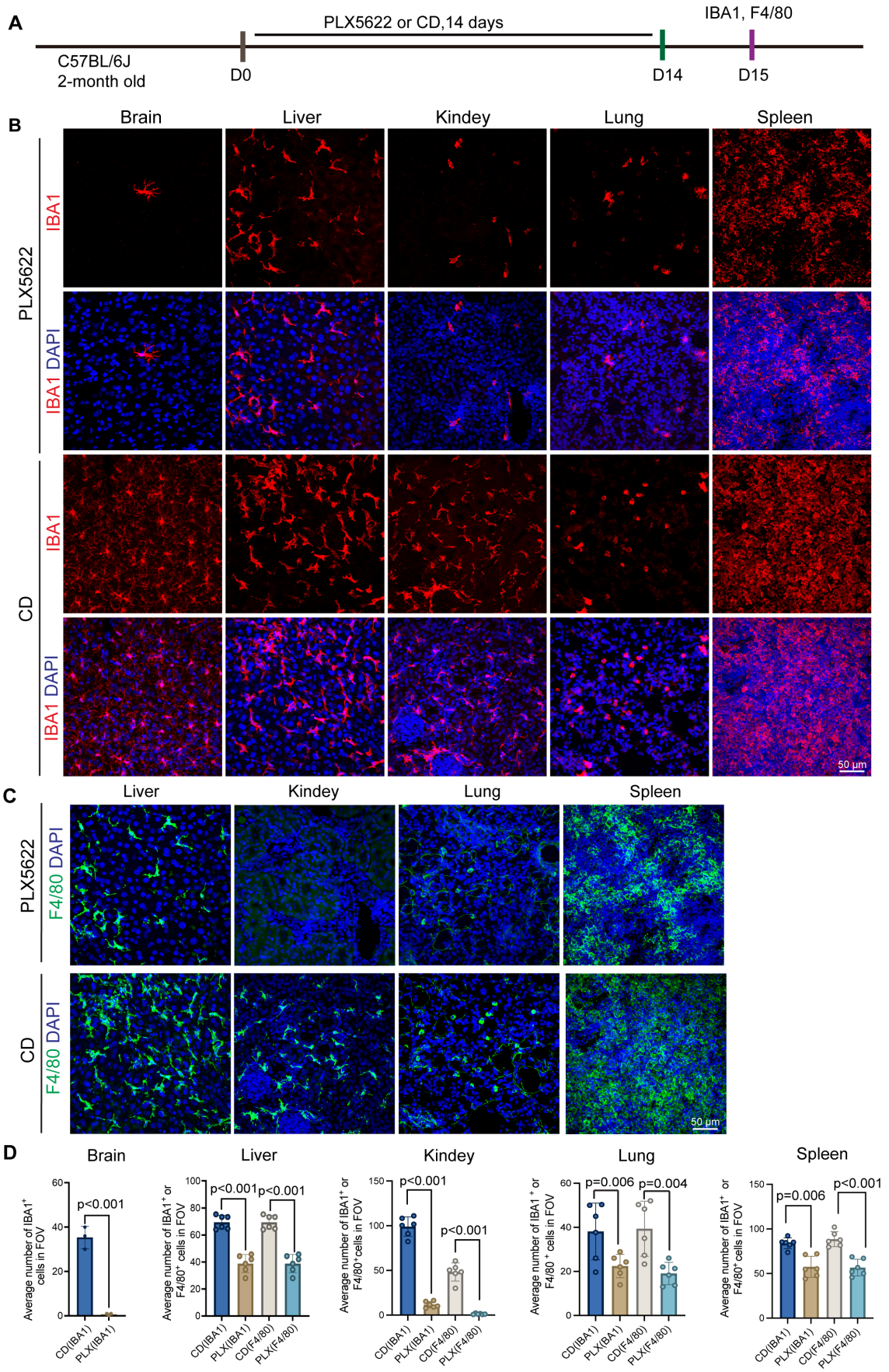

316 **Fig. 1 The CSF-1R antagonist, PLX5622, depleted microglia in the brain and resident**
317 **macrophages in peripheral tissue.** (A) Scheme of time points for microglial depletion and
318 examination time points. (B) Representative images show the depletion efficiency of microglia (IBA1,
319 red) in the brain or peripheral macrophages (IBA1, red) in the peripheral organs following the
320 administration of CD or PLX5622. Scale bar, 50 μm. (C) Representative images show the depletion
321 efficiency of tissue macrophages (F4/80, green) in peripheral organs following the administration of
322 PLX5622. Scale bar, 50 μm. (D) Quantification the average number of $IBA1^+$ cells or $F4/80^+$ cells in
323 the indicated organs. N = 3~6 mice. Two-tailed unpaired test. Data are presented as mean ± SD. CD:
324 control diet; FOV: Field of View; D: day.

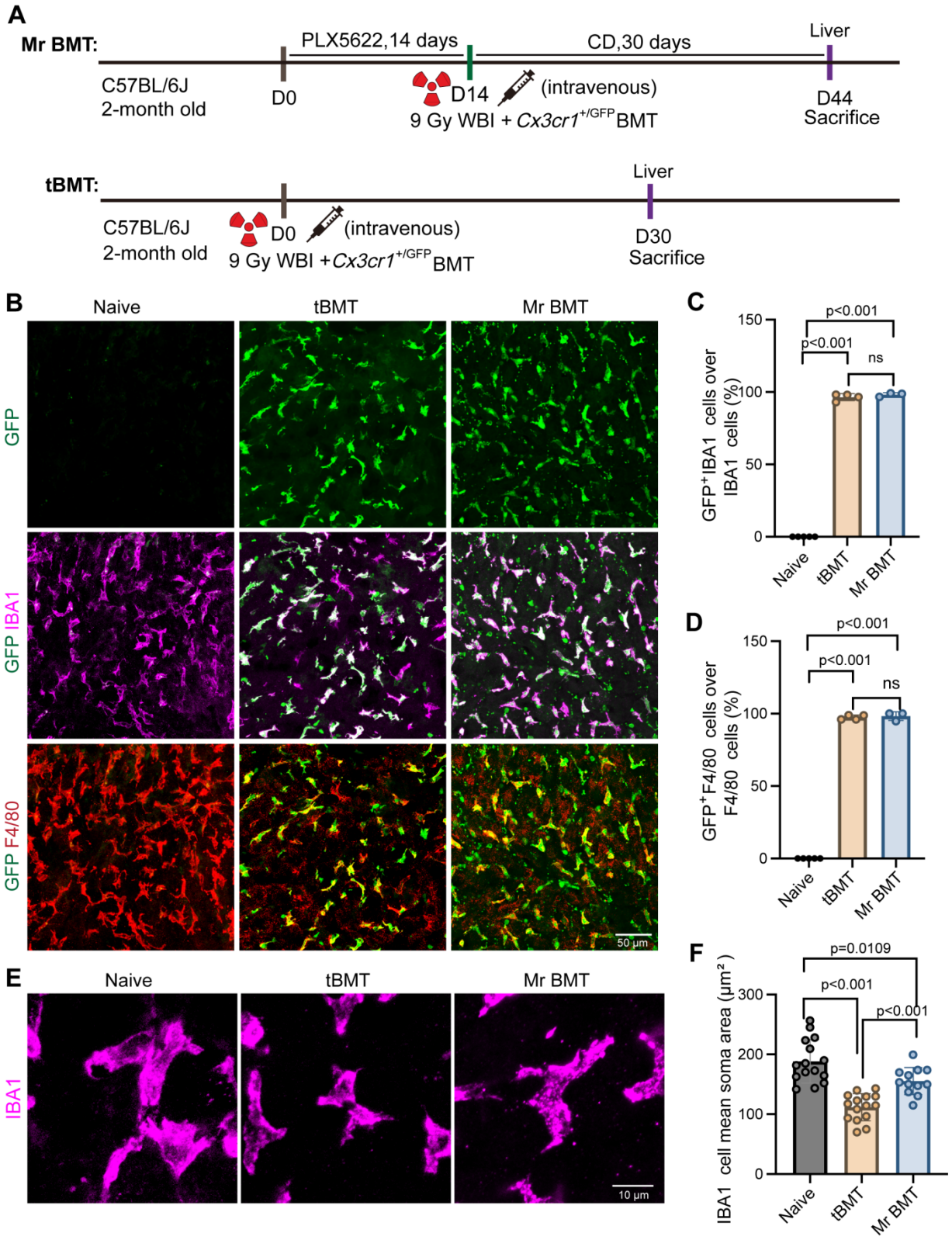

325

326 **Fig. 2 Mr BMT successfully replaced Kupffer cells with BM-derived macrophages in the liver.**

327 (A) Scheme of time points for Mr BMT and tBMT strategy. (B) Representative images show BM-

328 derived cells (GFP, green), liver resident macrophages (IBA1, magenta), liver resident macrophages

329 (F4/80, red) in the liver after tBMT or Mr BMT treatment. Scale bar, 50 μm. (C-D) Quantification the
330 percentage of tBMT-derived cells and Mr BMT-derived cells in the liver. N = 3~5 mice. One-way
331 ANOVA with Holm-Sidak multiple-comparisons test (post hoc). Data are presented as mean ± SD.
332 (E) Representative images show the morphology of BM-derived KCs (IBA1, magenta) in the liver.
333 Scale bar, 10um. (F) Quantification of soma area of $IBA1^+$ cells in the liver. N = 3~5 mice. For each
334 mouse, take three non-consecutive sections, and each dot represents one cell. Each dot represents one
335 cell. One-way ANOVA with Holm-Sidak multiple-comparisons test (post hoc). Data are presented as
336 mean ± SD. CD: control diet; WBI: whole brain irradiation; D: day.

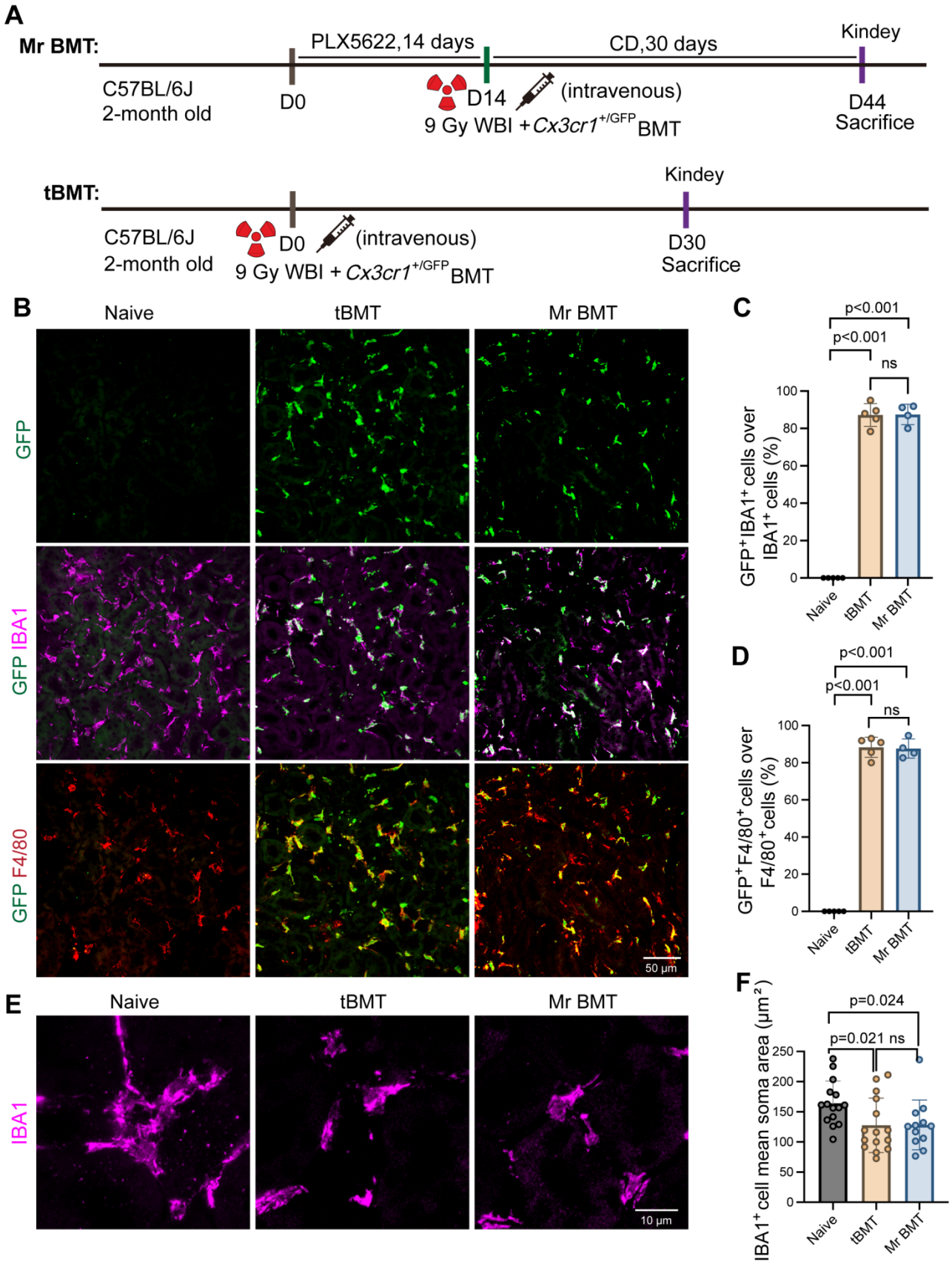
A
Mr BMT:
PLX5622,14 days
CD,30 days
Kindey
C57BL/6J
2-month old
D0
D14
(intravenous)
9 Gy WBI + Cx3cr1+/GFP BMT
D44
Sacrifice
tBMT:
Kindey
C57BL/6J
2-month old
D0
(intravenous)
9 Gy WBI + Cx3cr1+/GFP BMT
D30
Sacrifice
B
Naive
tBMT
Mr BMT
GFP
GFP IBA1
GFP F4/80
50 μm
C
p<0.001
p<0.001
ns
GFP+IBA1+ cells over IBA1+ cells (%)
Naive
tBMT
Mr BMT
D
p<0.001
p<0.001
ns
GFP+F4/80+cells over F4/80+cells (%)
Naive
tBMT
Mr BMT
E
Naive
tBMT
Mr BMT
IBA1
10 μm
F
p=0.024
p=0.021 ns
IBA1+cell mean soma area (μm2)
Naive
tBMT
Mr BMT

337

338 **Fig. 3 Evaluate the efficiency of the Mr BMT strategy in replacing macrophages in kidney.** (A)
339 Scheme of time points for Mr BMT and tBMT strategy. (B) Representative images show BM-derived
340 cells (GFP, green), kidney resident macrophages (IBA1, magenta), kidney resident macrophages
341 (F4/80, red) in the kideney after tBMT or Mr BMT treatment. Scale bar, 50 μm. (C-D) Quantification
342 the percentage of tBMT-derived cells or Mr BMT-derived cells in the kidney. N = 4~5 mice. One-way
343 ANOVA with Holm-Sidak multiple-comparisons test (post hoc). Data are presented as mean ± SD. (E)
344 Representative images showing the morphology of BM-derived kidney macrophages (IBA1, magenta)
345 in the kidney. Scale bar, 10 μm. (F) Quantification of soma area of $IBA1^{+}$ cells in the kidney. N = 4~5
346 mice. For each mouse, take three non-consecutive sections, and each dot represents one cell. Each dot
347 represents one cell. One-way ANOVA with Holm-Sidak multiple-comparisons test (post hoc). Data
348 are presented as mean ± SD. CD: control diet; WBI: whole brain irradiation; D: day.

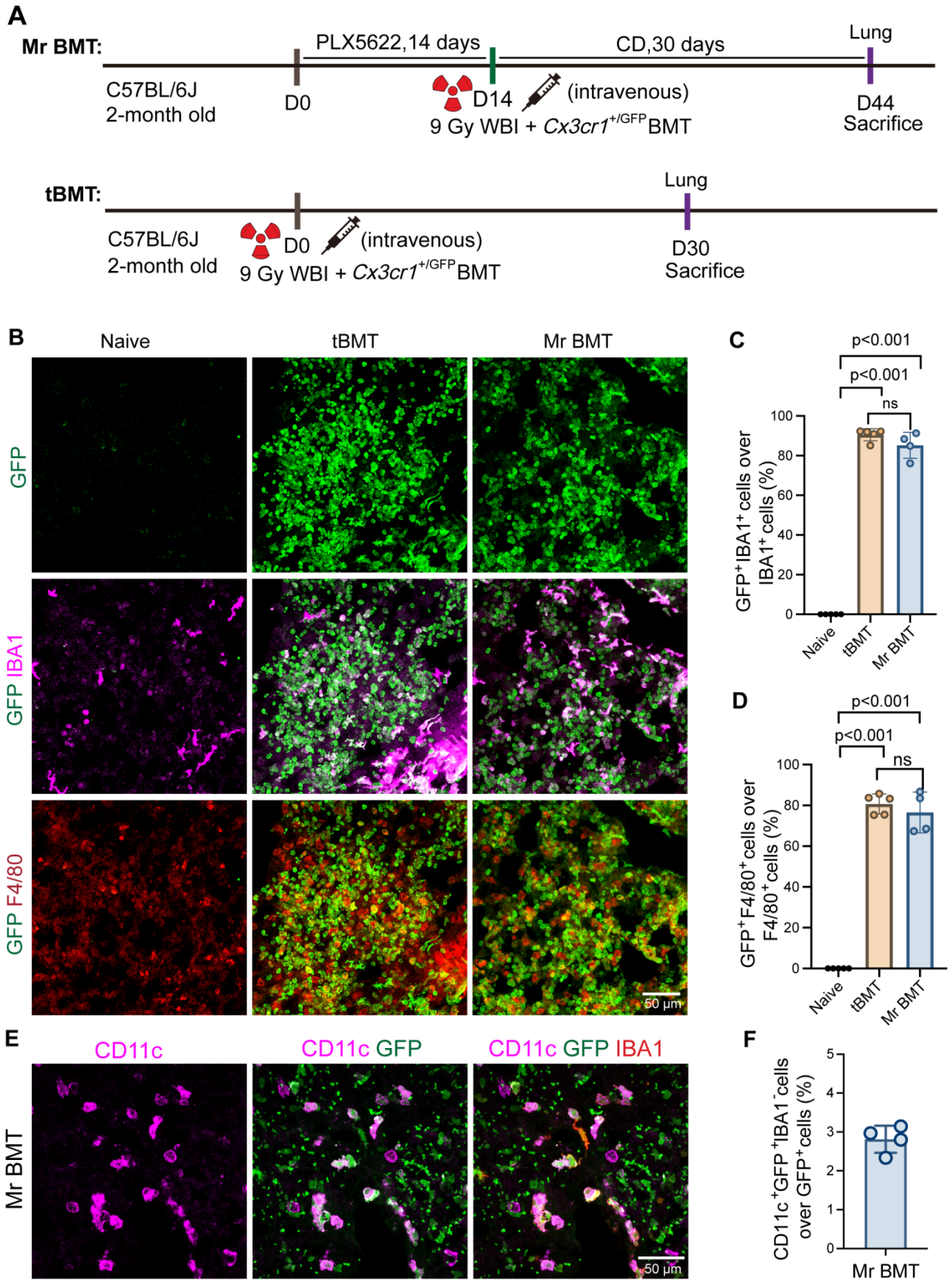
A
Mr BMT:
PLX5622,14 days
CD,30 days
Lung
C57BL/6J
2-month old
D0
D14
(intravenous)
9 Gy WBI + Cx3cr1+/GFP BMT
D44
Sacrifice
tBMT:
Lung
C57BL/6J
2-month old
D0
(intravenous)
9 Gy WBI + Cx3cr1+/GFP BMT
D30
Sacrifice
B
Naive
tBMT
Mr BMT
GFP
GFP IBA1
GFP F4/80
50 μm
C
p<0.001
p<0.001
ns
GFP+IBA1+ cells over IBA1+ cells (%)
Naive
tBMT
Mr BMT
D
p<0.001
p<0.001
ns
GFP+F4/80+ cells over F4/80+ cells (%)
Naive
tBMT
Mr BMT
E
CD11c
CD11c GFP
CD11c GFP IBA1
Mr BMT
50 μm
F
CD11c+GFP+IBA1- cells over GFP+ cells (%)
Mr BMT

349

350 **Fig. 4 Evaluate the replacement efficiency of lung tissue-resident macrophages under Mr BMT**
351 **treatmet.** (A) Scheme of time points for Mr BMT and tBMT strategy. (B) Representative images
352 show BM-derived cells (GFP, green), lung resident macrophages (IBA1, magenta), lung resident
353 macrophages (F4/80, red) in the lung after tBMT or Mr BMT treatment. Scale bar, 50 μm. (C-D)
354 Quantification the percentage of tBMT-derived cells or Mr BMT-derived cells in the lung. N = 4~5
355 mice. One-way ANOVA with Holm-Sidak multiple-comparisons test (post hoc). Data are presented
356 as mean ± SD. (E) Representative images show myeloid cells (CD11c, magenta), BM-derived cells
357 (GFP, green) and lung tissue-resident macrophages (IBA1, red) in the lung after Mr BMT. Scale bar,
358 50 μm. (F) Quantification the ratio of $CD11c^{+}$ GFP^{+} $IBA1^{-}$ cells / GFP^{+} cells in the lung after Mr BMT.
359 N = 4 mice. Data are presented as mean ± SD. CD: control diet; WBI: whole brain irradiation; D: day.

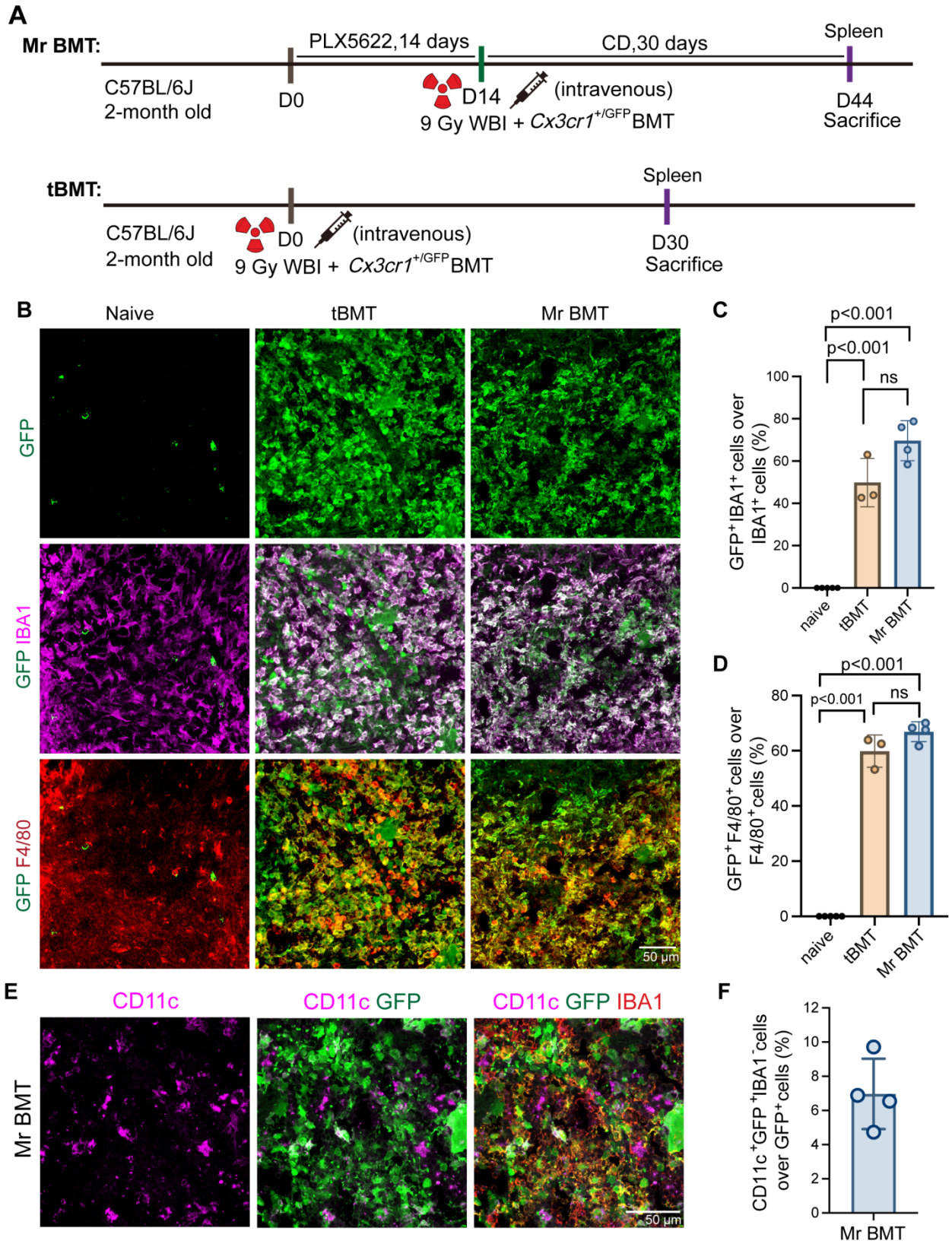

360

361 **Fig. 5 Replacement efficiency of spleen tissue-resident macrophages under Mr BMT treatmet.**

362 (A) Scheme of time points for Mr BMT and tBMT strategy. (B) Representative images show BM-

363 derived cells (GFP, green), spleen resident macrophages (IBA1, magenta), spleen resident
364 macrophages (F4/80, red) in the liver after tBMT or Mr BMT treatment. Scale bar, 50 μm. (C-D)
365 Quantification the percentage of tBMT-derived cell or Mr BMT cell percentage in the spleen. N = 3~5
366 mice. One-way ANOVA with Holm-Sidak multiple-comparisons test (post hoc). Data are presented
367 as mean ± SD. (E) Representative images show myeloid cells (CD11c, magenta), BM-derived cells
368 (GFP, green) and spleen tissue-resident macrophages (IBA1, red) in the spleen after Mr BMT. Scale
369 bar, 50 μm. (F) Quantification the ratio of $CD11c^{+}$ GFP^{+} $IBA1^{-}$ cells / GFP^{+} cells in the spleen after Mr
370 BMT. N = 4 mice. Data are presented as mean ± SD. CD: control diet; WBI: whole brain irradiation;
371 D: day.

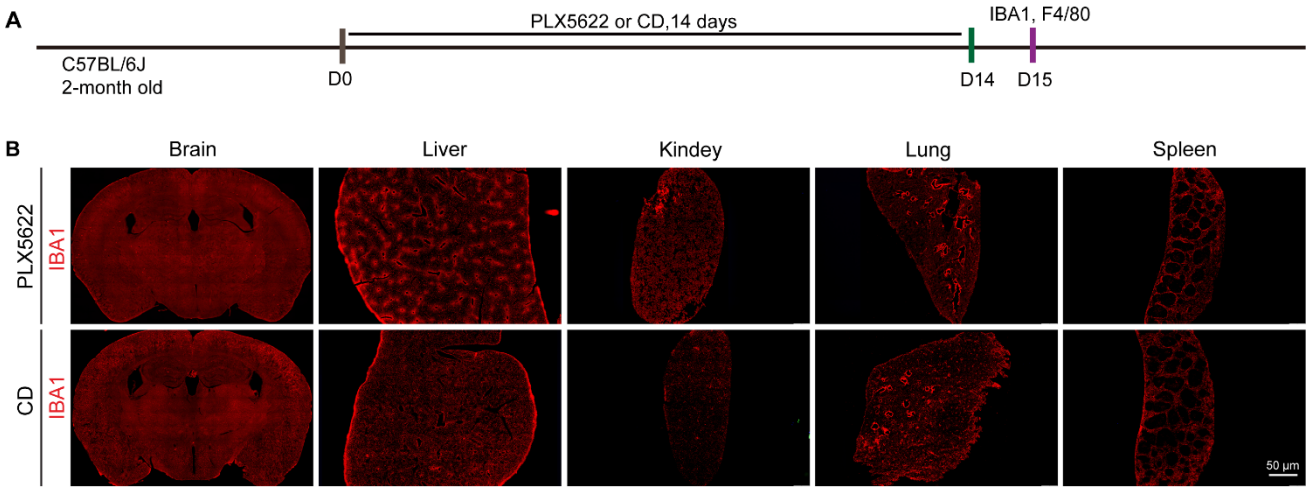

372

373 **Fig. S1 PLX5622 depleted microglia in CNS and resident macrophages in peripheral organs.** (A)
374 Scheme of time points for microglial depletion and examination time points. (B) Representative
375 images show the depletion efficiency of microglia (IBA1, red) in the whole brain or macrophages
376 (IBA1, red) in the peripheral organs following the administration of CD or PLX5622. Scale bar, 50
377 μm. CD: control diet; D: day.

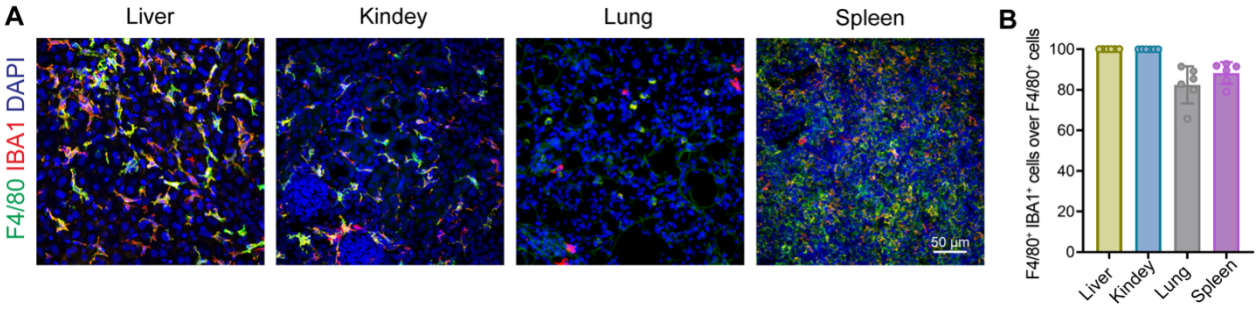

Fig. S2 The co-lable rate of F4/80 and IBA1 in peripheral tissues. (A) Representative images show the co-labeling of F4/80 and IBA1 in the peripheral organs of naïve group. (B) Quantification the percentage of $F4/80^{+}$ $IBA1^{+}$ cells over $IBA1^{+}$ cells in different peripheral tissues. N = 6 mice. Data are presented as mean ± SD. Scale bar, 50 μm.

383

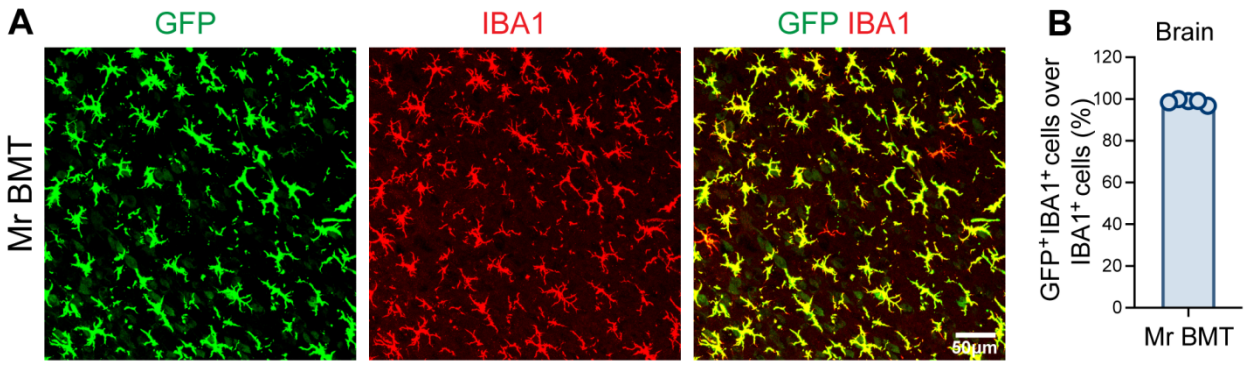

384

385 **Fig. S3 The replacement efficiency of Mr BMT in the brain was higher than in peripheral.** (A)
386 Representative images show the engrafted BM-derived microglia-like cells (GFP, green) in the brain
387 after Mr BMT. Scale bar, 50 μm. (B) Quantification the percentage of Mr BMT-derived cells in the
388 brain. N =5 mice. Data are presented as mean ± SD.

389

390

391

392

393

394

395

396

397

398

399

400

401

402

403 ***References***

404 1. Epelman S, Lavine KJ, Randolph GJ. Origin and functions of tissue macrophages. *Immunity*
405 2014; **41**(1)**:** 21-35. e-pub ahead of print 2014/07/19; doi: 10.1016/j.immuni.2014.06.013

406 2. Ginhoux F, Guilliams M. Tissue-Resident Macrophage Ontogeny and Homeostasis. *Immunity*
407 2016; **44**(3)**:** 439-449. e-pub ahead of print 2016/03/18; doi: 10.1016/j.immuni.2016.02.024

408 3. Hashimoto D, Chow A, Noizat C, Teo P, Beasley MB, Leboeuf M *et al.* Tissue-resident
409 macrophages self-maintain locally throughout adult life with minimal contribution from
410 circulating monocytes. *Immunity* 2013; **38**(4)**:** 792-804. e-pub ahead of print 2013/04/23; doi:
411 10.1016/j.immuni.2013.04.004

412 4. Wynn TA, Chawla A, Pollard JW. Macrophage biology in development, homeostasis and
413 disease. *Nature* 2013; **496**(7446)**:** 445-455. e-pub ahead of print 2013/04/27; doi:
414 10.1038/nature12034

415 5. Fischer A. Thirty years of bone marrow transplantation for severe combined immunodeficiency.
416 *The New England journal of medicine* 1999; **340**(7)**:** 559-561. e-pub ahead of print 1999/02/18;
417 doi: 10.1056/nejm199902183400711

418 6. Levite M, Zinger H, Zisman E, Reisner Y, Mozes E. Beneficial effects of bone marrow
419 transplantation on the serological manifestations and kidney pathology of experimental
420 systemic lupus erythematosus. *Cellular immunology* 1995; **162**(1)**:** 138-145. e-pub ahead of
421 print 1995/04/15; doi: 10.1006/cimm.1995.1061

422 7. Kushida T, Ueda Y, Umeda M, Oe K, Okamoto N, Iida H *et al.* Allogeneic intra-bone marrow
423 transplantation prevents rheumatoid arthritis in SKG/Jcl mice. *Journal of autoimmunity* 2009;
424 **32**(3-4)**:** 216-222. e-pub ahead of print 2009/04/08; doi: 10.1016/j.jaut.2009.02.015

425 8. Zhang S, Dai Q, Zhang B, Liu S, Wang Y, Zhang Y *et al.* Syngeneic bone marrow
426 transplantation in combination with PI3K inhibitor reversed hyperglycemia in later-stage

427 streptozotocin-induced diabetes. *Annals of translational medicine* 2021; **9**(22)**:** 1642. e-pub
428 ahead of print 2022/01/07; doi: 10.21037/atm-21-3329
429 9. Boffa G, Signori A, Massacesi L, Mariottini A, Sbragia E, Cottone S *et al.* Hematopoietic Stem
430 Cell Transplantation in People With Active Secondary Progressive Multiple Sclerosis.
431 *Neurology* 2023; **100**(11)**:** e1109-e1122. e-pub ahead of print 2022/12/22; doi:
432 10.1212/wnl.0000000000206750
433 10. Xu Z, Rao Y, Huang Y, Zhou T, Feng R, Xiong S *et al.* Efficient Strategies for Microglia
434 Replacement in the Central Nervous System. *Cell reports* 2020; **33**(8)**:** 108443. e-pub ahead of
435 print 2020/11/26; doi: 10.1016/j.celrep.2020.108443
436 11. Xu Z, Zhou X, Peng B, Rao Y. Microglia replacement by bone marrow transplantation (Mr
437 BMT) in the central nervous system of adult mice. *STAR protocols* 2021; **2**(3)**:** 100666. e-pub
438 ahead of print 2021/07/22; doi: 10.1016/j.xpro.2021.100666
439 12. Xu Z, Rao Y, Peng B. Protocol for microglia replacement by peripheral blood (Mr PB). *STAR*
440 *protocols* 2021; **2**(2)**:** 100613. e-pub ahead of print 2021/06/29; doi:
441 10.1016/j.xpro.2021.100613
442 13. Yoo Y, Neumayer G, Shibuya Y, Mader MM, Wernig M. A cell therapy approach to restore
443 microglial Trem2 function in a mouse model of Alzheimer's disease. *Cell stem cell* 2023; **30**(8)**:**
444 1043-1053.e1046. e-pub ahead of print 2023/08/05; doi: 10.1016/j.stem.2023.07.006
445 14. Shibuya Y, Kumar KK, Mader MM, Yoo Y, Ayala LA, Zhou M *et al.* Treatment of a genetic
446 brain disease by CNS-wide microglia replacement. *Science translational medicine* 2022;
447 **14**(636)**:** eabl9945. e-pub ahead of print 2022/03/17; doi: 10.1126/scitranslmed.abl9945
448 15. Colella P, Sayana R, Suarez-Nieto MV, Sarno J, Nyame K, Xiong J *et al.* CNS Repopulation
449 by Hematopoietic-Derived Microglia-Like Cells Corrects Progranulin deficiency. *Research*
450 *square* 2023. e-pub ahead of print 2023/10/04; doi: 10.21203/rs.3.rs-3263412/v1
451 16. Manickam V, Gawande DY, Stothert AR, Clayman AC, Batalkina L, Warchol ME *et al.*

452 Macrophages Promote Repair of Inner Hair Cell Ribbon Synapses following Noise-Induced
453 Cochlear Synaptopathy. *The Journal of neuroscience : the official journal of the Society for*
454 *Neuroscience* 2023; **43**(12)**:** 2075-2089. e-pub ahead of print 2023/02/23; doi:
455 10.1523/jneurosci.1273-22.2023
456 17. Li Y, Ritzel RM, Khan N, Cao T, He J, Lei Z *et al.* Delayed microglial depletion after spinal
457 cord injury reduces chronic inflammation and neurodegeneration in the brain and improves
458 neurological recovery in male mice. *Theranostics* 2020; **10**(25)**:** 11376-11403. e-pub ahead of
459 print 2020/10/15; doi: 10.7150/thno.49199
460 18. Spiteri AG, Ni D, Ling ZL, Macia L, Campbell IL, Hofer MJ *et al.* PLX5622 Reduces Disease
461 Severity in Lethal CNS Infection by Off-Target Inhibition of Peripheral Inflammatory
462 Monocyte Production. *Frontiers in immunology* 2022; **13:** 851556. e-pub ahead of print
463 2022/04/12; doi: 10.3389/fimmu.2022.851556
464 19. Jung S, Aliberti J, Graemmel P, Sunshine MJ, Kreutzberg GW, Sher A *et al.* Analysis of
465 fractalkine receptor CX(3)CR1 function by targeted deletion and green fluorescent protein
466 reporter gene insertion. *Mol Cell Biol* 2000; **20**(11)**:** 4106-4114. e-pub ahead of print
467 2000/05/11; doi: 10.1128/mcb.20.11.4106-4114.2000
468 20. Brochu S, Perreault C, Bélanger R. Evaluation of Fc-dependent monocyte-macrophage
469 function in bone marrow transplant recipients. *Experimental hematology* 1989; **17**(9)**:** 948-951.
470 e-pub ahead of print 1989/10/01;
471 21. Hume DA, MacDonald KP. Therapeutic applications of macrophage colony-stimulating factor-
472 1 (CSF-1) and antagonists of CSF-1 receptor (CSF-1R) signaling. *Blood* 2012; **119**(8)**:** 1810-
473 1820. e-pub ahead of print 2011/12/22; doi: 10.1182/blood-2011-09-379214
474 22. Stanley ER, Chitu V. CSF-1 receptor signaling in myeloid cells. *Cold Spring Harbor*
475 *perspectives in biology* 2014; **6**(6). e-pub ahead of print 2014/06/04; doi:
476 10.1101/cshperspect.a021857

477 23. Huang Y, Xu Z, Xiong S, Sun F, Qin G, Hu G *et al.* Repopulated microglia are solely derived
478 from the proliferation of residual microglia after acute depletion. *Nature neuroscience* 2018;
479 **21**(4)**:** 530-540. e-pub ahead of print 2018/02/24; doi: 10.1038/s41593-018-0090-8
480 24. Rojo R, Raper A, Ozdemir DD, Lefevre L, Grabert K, Wollscheid-Lengeling E *et al.* Deletion
481 of a Csf1r enhancer selectively impacts CSF1R expression and development of tissue
482 macrophage populations. *Nature communications* 2019; **10**(1)**:** 3215. e-pub ahead of print
483 2019/07/22; doi: 10.1038/s41467-019-11053-8
484 25. Arreola MA, Soni N, Crapser JD, Hohsfield LA, Elmore MRP, Matheos DP *et al.* Microglial
485 dyshomeostasis drives perineuronal net and synaptic loss in a CSF1R(+/-) mouse model of
486 ALSP, which can be rescued via CSF1R inhibitors. *Science advances* 2021; **7**(35). e-pub ahead
487 of print 2021/08/27; doi: 10.1126/sciadv.abg1601
488 26. Spangenberg E, Severson PL, Hohsfield LA, Crapser J, Zhang J, Burton EA *et al.* Sustained
489 microglial depletion with CSF1R inhibitor impairs parenchymal plaque development in an
490 Alzheimer's disease model. *Nature communications* 2019; **10**(1)**:** 3758. e-pub ahead of print
491 2019/08/23; doi: 10.1038/s41467-019-11674-z
492 27. Wächter C, Eiden LE, Naumann N, Depboylu C, Weihe E. Loss of cerebellar neurons in the
493 progression of lentiviral disease: effects of CNS-permeant antiretroviral therapy. *Journal of*
494 *neuroinflammation* 2016; **13**(1)**:** 272. e-pub ahead of print 2016/10/16; doi: 10.1186/s12974-
495 016-0726-0
496 28. Leenen PJ, Radosević K, Voerman JS, Salomon B, van Rooijen N, Klatzmann D *et al.*
497 Heterogeneity of mouse spleen dendritic cells: in vivo phagocytic activity, expression of
498 macrophage markers, and subpopulation turnover. *Journal of immunology (Baltimore, Md. :*
499 *1950)* 1998; **160**(5)**:** 2166-2173. e-pub ahead of print 1998/03/14;
500 29. Lenda DM, Kikawada E, Stanley ER, Kelley VR. Reduced macrophage recruitment,
501 proliferation, and activation in colony-stimulating factor-1-deficient mice results in decreased

502 tubular apoptosis during renal inflammation. *Journal of immunology (Baltimore, Md. : 1950)*
503 2003; **170**(6)**:** 3254-3262. e-pub ahead of print 2003/03/11; doi: 10.4049/jimmunol.170.6.3254
504 30. McCowan J, Fercoq F, Kirkwood PM, T'Jonck W, Hegarty LM, Mawer CM *et al.* The
505 transcription factor EGR2 is indispensable for tissue-specific imprinting of alveolar
506 macrophages in health and tissue repair. *Science immunology* 2021; **6**(65)**:** eabj2132. e-pub
507 ahead of print 2021/11/20; doi: 10.1126/sciimmunol.abj2132
508 31. Bonfield TL, Thomassen MJ, Farver CF, Abraham S, Koloze MT, Zhang X *et al.* Peroxisome
509 proliferator-activated receptor-gamma regulates the expression of alveolar macrophage
510 macrophage colony-stimulating factor. *Journal of immunology (Baltimore, Md. : 1950)* 2008;
511 **181**(1)**:** 235-242. e-pub ahead of print 2008/06/21; doi: 10.4049/jimmunol.181.1.235
512 32. Rietkötter E, Bleckmann A, Bayerlová M, Menck K, Chuang HN, Wenske B *et al.* Anti-CSF-
513 1 treatment is effective to prevent carcinoma invasion induced by monocyte-derived cells but
514 scarcely by microglia. *Oncotarget* 2015; **6**(17)**:** 15482-15493. e-pub ahead of print 2015/06/23;
515 doi: 10.18632/oncotarget.3855
516 33. Ide S, Yahara Y, Kobayashi Y, Strausser SA, Ide K, Watwe A *et al.* Yolk-sac-derived
517 macrophages progressively expand in the mouse kidney with age. *eLife* 2020; **9**. e-pub ahead
518 of print 2020/04/18; doi: 10.7554/eLife.51756
519 34. Mass E, Ballesteros I, Farlik M, Halbritter F, Günther P, Crozet L *et al.* Specification of tissue-
520 resident macrophages during organogenesis. *Science (New York, N.Y.)* 2016; **353**(6304). e-pub
521 ahead of print 2016/08/06; doi: 10.1126/science.aaf4238
522 35. Ginhoux F, Greter M, Leboeuf M, Nandi S, See P, Gokhan S *et al.* Fate mapping analysis
523 reveals that adult microglia derive from primitive macrophages. *Science (New York, N.Y.)* 2010;
524 **330**(6005)**:** 841-845. e-pub ahead of print 2010/10/23; doi: 10.1126/science.1194637
525 36. Hubbard LL, Wilke CA, White ES, Moore BB. PTEN limits alveolar macrophage function
526 against Pseudomonas aeruginosa after bone marrow transplantation. *American journal of*

527 *respiratory cell and molecular biology* 2011; **45**(5)**:** 1050-1058. e-pub ahead of print
528 2011/04/30; doi: 10.1165/rcmb.2011-0079OC
529 37. Chiot A, Zaïdi S, Iltis C, Ribon M, Berriat F, Schiaffino L *et al.* Modifying macrophages at the
530 periphery has the capacity to change microglial reactivity and to extend ALS survival. *Nature*
531 *neuroscience* 2020; **23**(11)**:** 1339-1351. e-pub ahead of print 2020/10/21; doi: 10.1038/s41593-
532 020-00718-z
533 38. Jakubzick C, Tacke F, Ginhoux F, Wagers AJ, van Rooijen N, Mack M *et al.* Blood monocyte
534 subsets differentially give rise to CD103+ and CD103- pulmonary dendritic cell populations.
535 *Journal of immunology (Baltimore, Md. : 1950)* 2008; **180**(5)**:** 3019-3027. e-pub ahead of print
536 2008/02/23; doi: 10.4049/jimmunol.180.5.3019
537 39. del Rio ML, Rodriguez-Barbosa JI, Bölter J, Ballmaier M, Dittrich-Breiholz O, Kracht M *et al.*
538 CX3CR1+ c-kit+ bone marrow cells give rise to CD103+ and CD103- dendritic cells with
539 distinct functional properties. *Journal of immunology (Baltimore, Md. : 1950)* 2008; **181**(9)**:**
540 6178-6188. e-pub ahead of print 2008/10/23; doi: 10.4049/jimmunol.181.9.6178
541 40. Aegerter H, Lambrecht BN, Jakubzick CV. Biology of lung macrophages in health and disease.
542 *Immunity* 2022; **55**(9)**:** 1564-1580. e-pub ahead of print 2022/09/15; doi:
543 10.1016/j.immuni.2022.08.010
544 41. Yu YR, Hotten DF, Malakhau Y, Volker E, Ghio AJ, Noble PW *et al.* Flow Cytometric Analysis
545 of Myeloid Cells in Human Blood, Bronchoalveolar Lavage, and Lung Tissues. *Am J Respir*
546 *Cell Mol Biol* 2016; **54**(1)**:** 13-24. e-pub ahead of print 2015/08/13; doi: 10.1165/rcmb.2015-
547 0146OC
548 42. Todd EM, Zhou JY, Szasz TP, Deady LE, D'Angelo JA, Cheung MD *et al.* Alveolar
549 macrophage development in mice requires L-plastin for cellular localization in alveoli. *Blood*
550 2016; **128**(24)**:** 2785-2796. e-pub ahead of print 2016/10/21; doi: 10.1182/blood-2016-03-
551 705962

552